Effect of a two-phase wedge-sliding model on the ingredient drift of a stable mixed fluid and its computing method*

Han Zhi-Hong(韩志宏)† and Liu Zuo-Min(刘佐民)

Tribological Institute, Wuhan University of Technology, Wuhan 430070*, China*

(Received 10 August 2011; revised manuscript received 13 October 2011)

A two-phase wedge-sliding model is developed based on the micro-cellular structure and minimum entropy theory of a stable system, and it is used to describe the ingredient distribution of a mixed fluid in a non-uniform stress field and to analyse its phase drift phenomenon. In the model, the drift–inhibition angle and the expansion–inhibition angle are also deduced and used as evaluating indexes to describe the drifting trend of different ingredients among the mixed fluids. For solving above two indexes of the model, a new calculation method is developed and used to compute the phase distributions of multiphase fluid at peak stress and gradient area stress, respectively. As an example, the flow process of grease in a pipe is analysed by simulation method and used to verify the validity of the model.

Keywords: mixed fluid, ingredient drift, wedge-sliding model, computing method

PACS: 47.20.–k, 47.61.Jd, 64.75.Cd, 83.60.Wc **DOI:** 10.1088/1674-1056/21/8/084701

1. Introduction

Mixed fluid is widely used in industry to solve some engineering problems, such as loading bearing, lubrication, vibration attenuation, and so on. However, the separation and sediment process of ingredients of a mixed fluid is a multi-scale and multi-factor coupling, and its rheological properties is very complicated. Especially when mixed fluid in a micro-particle-added lubricant is used in porous material, it is difficult to analyse the inner ingredient distribution of mixed fluid and to describe the contribution of the physical characteristics of each phase in the fluid to lubricating film thickness and resistant pressure capacity.

Up to now, many studies[1−5] have supported that the shear thinning and the drift of heavier phase in a mixed fluid in a non-uniform stress field is a universal phenomenon. Due to the fact that different mixed fluids usually have different ingredients and loading conditions, some appropriate improvements always need to be made when a model is used to describe its rheological characteristics.[6−9] However, because of the coupling of different resulting physical phenomena of the multi-phase flow, the present models seem to be still lacking in describing the deformation of the internal structure, the mass transport, and the ingredient distribution in the mixed fluid. Furthermore, there are few reports on the flow models which are devoted to the problems of the ingredient separation and inner distribution of different phases in mixed fluid. In addition, in most of the models[10−13] the viscosity of mixed fluid was taken as an important parameter, but there is no evidence showing that the ingredient distribution in mixed fluid at a long-term steady-state is related to the viscosity of fluid.

So it is not suitable to accurately describe the inner ingredient distribution of mixed fluid by using some existing two-phase flow models, and a new method needs to be developed.

Furthermore, a model involving more complex coupling factors, and a fast and reasonable computing method is more important for its practical application. Many successful attempts[14−16] have been suggested to model the rheology of multi-phase fluid: these are the results of the applications of current computer technology and advanced research method in the research field of multi-phase fluids.

The purposes of this work are to put forward a feasible multi-phase flow model to describe the ingredient separation in non-uniform stress field and inner distribution of different phases in a mixed fluid in a

*Project supported by the National Natural Science Foundation of China (Grant No. 51075311).

†Corresponding author. E-mail: handled@sina.cn

© 2012 Chinese Physical Society and IOP Publishing Ltd

long-term steady state; to study its relevant influence factors of the model and analyse the changing regularities of those factors; to present a fast and reasonable solving method for the model and its computing steps in detail; and finally to take the flow of grease in pipe as an example to test the validity of the model by calculation and simulation correspondingly.

2. Design of the drift model

2.1. Two-phase wedge-sliding cell

Extracting a micro cell anywhere in the mixed fluid and assuming the faying surface of two phases to occur at a wedge, as shown in Fig. 1.

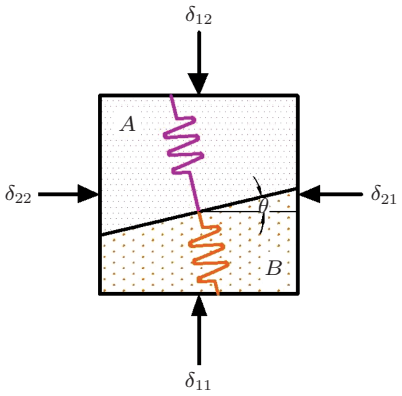


Fig. 1. (colour online) A two-phase wedge-sliding cell.

In Fig. 1, A and B respectively denote the lighter and the heavier phases of the cell; δ_{12} and δ_{11} are the longitudinal stress pair (N/mm^2) and δ_{22} and δ_{21} the transverse stress pair (N/mm^2); θ is the wedge angle ($^\circ$) and $\theta \in (-\pi/2, +\pi/2)$.

Defining both the densities of two ingredients and their volume ratios in the mixed fluid as ρ_A, ρ_B (g/mm^3), and Φ_A, Φ_B and defining the volume ratios of phases A and B in cell as ϕ_A and ϕ_B, then there are apparently the following equations:

$$\Phi_A + \Phi_B = 1 \quad \text{and} \quad \phi_A + \phi_B = 1.$$

According to the theory of material mechanics, a pressurant has a tendency to reduce the force on an unit area by increasing its actual bearing surface, and the softer the material, the bigger the actual bearing area after deformation is. Assume that the two phases in a cell are both elastic-plastic bodies, and the actual bearing stress of each phase is proportional to its mass in cell, then the inner anti-forces of both phases under pressure can be defined as follows:

$$\begin{aligned} F_{kA} &= \lambda_k \zeta_{cA} m_{cA} \psi_p \\ &= \lambda_k \frac{\rho_A V_c \phi_A}{\rho_A V_c \phi_A + \rho_B V_c \phi_B} \\ &\quad \times \rho_A \phi_A V_c \frac{\mathrm{e}^{\lambda_\delta \delta_y} - \mathrm{e}^{-\lambda_\delta \delta_y}}{\mathrm{e}^{\lambda_\delta \delta_y} + \mathrm{e}^{-\lambda_\delta \delta_y}} \\ &= \lambda_k \frac{\rho_A^2 \phi_A^2}{\rho_A \phi_A + \rho_B \phi_B} \frac{\mathrm{e}^{\lambda_\delta \delta_y} - \mathrm{e}^{-\lambda_\delta \delta_y}}{\mathrm{e}^{\lambda_\delta \delta_y} + \mathrm{e}^{-\lambda_\delta \delta_y}}, \end{aligned} \tag{1}$$

$$\begin{aligned} F_{kB} &= \lambda_k \zeta_{cB} m_{cB} \psi_p \\ &= \lambda_k \frac{\rho_B V_c \phi_B}{\rho_A V_c \phi_A + \rho_B V_c \phi_B} \\ &\quad \times \rho_B \phi_B V_c \frac{\mathrm{e}^{\lambda_\delta \delta_y} - \mathrm{e}^{-\lambda_\delta \delta_y}}{\mathrm{e}^{\lambda_\delta \delta_y} + \mathrm{e}^{-\lambda_\delta \delta_y}} \\ &= \lambda_k \frac{\rho_B^2 \phi_B^2}{\rho_A \phi_A + \rho_B \phi_B} \frac{\mathrm{e}^{\lambda_\delta \delta_y} - \mathrm{e}^{-\lambda_\delta \delta_y}}{\mathrm{e}^{\lambda_\delta \delta_y} + \mathrm{e}^{-\lambda_\delta \delta_y}}. \end{aligned} \tag{2}$$

The action line of the forces is perpendicular to the wedge surface. In Eqs. (1) and (2), F_{kA} and F_{kB} are, respectively, the inner anti-forces of each phase N$\cdot$mm^{-2}); λ_k is the elastic-plastic anti-force coefficient of cell (N $\cdot$ g $\cdot$ mm^{-2}); V_c is the volume of cell and $V_c = 1$ (mm^3) here; m_{cA}, m_{cB}, and ζ_{cA}, ζ_{cB} are, respectively, the mass (g) and the mass fraction of each phase, and these can be simply calculated as follows:

$$\begin{aligned} m_{cA} &= \rho_A \phi_A V_c = \rho_A \phi_A, \\ \zeta_{cA} &= \frac{\rho_A V_c \phi_A}{\rho_A V_c \phi_A + \rho_B V_c \phi_B} = \frac{\rho_A \phi_A}{\rho_A \phi_A + \rho_{Bc} \phi_B} \\ &= \frac{m_{cA}}{m_{cA} + m_{cB}}, \\ m_{cB} &= \rho_B \phi_B V_c = \rho_B \phi_B, \\ \zeta_{cB} &= \frac{\rho_B V_c \phi_B}{\rho_A V_c \phi_A + \rho_B V_c \phi_B} = \frac{\rho_B \phi_B}{\rho_A \phi_A + \rho_{Bc} \phi_B} \\ &= \frac{m_{cB}}{m_{cA} + m_{cB}}; \end{aligned}$$

ψ_p is the plastic deformation coefficient of cell, and considering the weak bonding action of fluid molecules, it is simply defined as

$$\psi_p = \frac{\mathrm{e}^{\lambda_\delta \delta_y} - \mathrm{e}^{-\lambda_\delta \delta_y}}{\mathrm{e}^{\lambda_\delta \delta_y} + \mathrm{e}^{-\lambda_\delta \delta_y}},$$

with δ_y being the loading force on cell (N/mm^2), λ_δ being the prior coefficient of power exponential and also indexing the transverse expansion of unit cube of fluid under pressure. According to the contact deformation theory and the mass distribution principle of the above forces, the function of λ_δ is constructed here as

$$\lambda_\delta = \frac{\mathrm{e}^{\rho_A \phi_A + \rho_B \phi_B}}{\mathrm{e}^{\rho_A \phi_A + \rho_B \phi_B} - 1}. \tag{3}$$

Clearly, $0 < \lambda_\delta < 1$ and λ_δ has no unit.

By adding Eqs. (1) and (2) and taking $F_{kA} + F_{kB} = \delta_y$, λ_k can be obtained as

$$\lambda_k = \delta_y \frac{\rho_A\varphi_A + \rho_B\varphi_B}{\rho_A^2\varphi_A^2 + \rho_B^2\varphi_B^2} \frac{\mathrm{e}^{\lambda_\delta\delta_y} + \mathrm{e}^{-\lambda_\delta\delta_y}}{\mathrm{e}^{\lambda_\delta\delta_y} - \mathrm{e}^{-\lambda_\delta\delta_y}}. \quad (4)$$

From the minimum entropy theory, the acting force on the wedge surface beween two phases is the maximum static friction force when the flow reaches its steady state, and it can be defined as

$$F_\mathrm{f} = \lambda_\mathrm{f}(F_{kA} + F_{kB}), \quad (5)$$

where the acting direction of F_f ($\mathrm{N/mm^2}$) is parallel to the wedge surface but opposite to the trend of movement; λ_f is the maximum static friction coefficient between two phases, which is related to the environmental temperature and pressure and assumed to be a constant here.

Substituting Eqs. (1) and (2) into Eq. (5), the following equation is obtained

$$F_\mathrm{f} = \lambda_\mathrm{f}\lambda_k \frac{\rho_B^2\phi_B^2 + \rho_B^2\phi_B^2}{\rho_A\phi_A + \rho_B\phi_B} \frac{\mathrm{e}^{\lambda_\delta\delta_y} + \mathrm{e}^{-\lambda_\delta\delta_y}}{\mathrm{e}^{\lambda_\delta\delta_y} - \mathrm{e}^{-\lambda_\delta\delta_y}}.$$

For the convenience of writing, the volume ratio of phase B in cell ϕ_B is renamed λ, then $\phi_A = 1 - \lambda$. Substituting ϕ_A and ϕ_B by λ, the above equation can be rewritten as

$$F_\mathrm{f} = \lambda_\mathrm{f}\lambda_k \frac{\rho_A^2(1-\lambda)^2 + \rho_B^2\lambda^2}{\rho_A(1-\lambda) + \rho_B\lambda)} \frac{\mathrm{e}^{\lambda_\delta\delta_y} + \mathrm{e}^{-\lambda_\delta\delta_y}}{\mathrm{e}^{\lambda_\delta\delta_y} - \mathrm{e}^{-\lambda_\delta\delta_y}}. \quad (6)$$

Defining

$$C_\rho = \frac{\rho_A^2(1-\lambda)^2 + \rho_B^2\lambda^2}{\rho_A(1-\lambda) + \rho_B\lambda}, \quad (7)$$

C_ρ can also be named the joint stress modulus of cell ($\mathrm{g \cdot mm^{-3}}$) since it indicates the effect of volume ratio of ingredients of the cell on the stability of mixed fluid under pressure. Assuming $\rho_B > \rho_A$, Eq. (7) can be expanded into

$$\begin{aligned} C_\rho = {} & \frac{\rho_B^2 + \rho_A^2}{(\rho_B - \rho_A)^2}[\rho_A + (\rho_B - \rho_A)\lambda] \\ & - \frac{2\rho_A\rho_B(\rho_B + \rho_A)}{(\rho_B - \rho_A)^2} + \frac{2\rho_B^2\rho_A^2}{(\rho_B - \rho_A)^2} \\ & \times \frac{1}{[\rho_A + (\rho_B - \rho_A)\lambda]}. \end{aligned} \quad (8)$$

By deriving once C_ρ with respect to λ, the following equation is obtained:

$$\begin{aligned} \frac{\mathrm{d}(C_\rho)}{\mathrm{d}\lambda} = {} & \frac{\rho_A^2 + \rho_B^2}{\rho_B - \rho_A} - \frac{2\rho_A^2\rho_B^2}{\rho_B - \rho_A} \\ & \times \frac{1}{[(\rho_B - \rho_A)\lambda + \rho_A]^2}. \end{aligned} \quad (9)$$

Substituting Eq. (7) into Eq. (6), the resulting equation can then be rewritten as

$$F_\mathrm{f} = \lambda_\mathrm{f}\lambda_k C_\rho \frac{\mathrm{e}^{\lambda_\delta\delta_{12}} - \mathrm{e}^{-\lambda_\delta\delta_{12}}}{\mathrm{e}^{\lambda_\delta\delta_{12}} + \mathrm{e}^{-\lambda_\delta\delta_{12}}}. \quad (10)$$

2.2. Stresses equilibrium analysis of two-phase flow in a slot

The mixed fluid is assumed to steadily flow in a slot, which is caused by the uniform pressure difference $\Delta P = P_1 - P_2$, where P_1 and P_2 are the pressures respectively at two ends (Pa) as shown in Fig. 2(a).

Some assumptions were made as follows in order to simplify analysis: (i) two phases distribute uniformly in the mixed fluid initially; (ii) no gravity is taken into consideration; (iii) the slot is completely rigid; (iv) no deformation of fluid in the direction perpendicular to the flow is taken into account; (v) ambient temperature and pressure are both kept unchanged.

Taking the heavier phase for example, and building the coordinate in the wedge surface as shown in Fig. 3, the equilibrium equations are obtained as follows: in the direction parallel to the wedge surface,

$$(\delta_{12} - \delta_{11})\sin\theta + (\delta_{22} - \delta_{21})\cos\theta - F_\mathrm{f} = 0, \quad (11)$$

in the direction perpendicular to the wedge surface,

$$\begin{aligned} & (\delta_{12} - \delta_{11})\cos\theta + (\delta_{22} - \delta_{21})\sin\theta \\ & - (F_{kA} + F_{kB}) = 0. \end{aligned} \quad (12)$$

The longitudinal pressure difference and the transverse expansion–inhibition force, respectively, are

$$\delta = \frac{\Delta p}{A_p} = \delta_{12} - \delta_{11}, \quad (13)$$

$$C_h = \delta_{21} - \delta_{22}, \quad (14)$$

where A_p is the transverse surface area of the fluid in slot ($\mathrm{mm^2}$).

Substituting Eqs. (10), (13), and (14) into Eq. (11), the following equation is obtained

$$\delta\sin\theta - C_h\cos\theta = \lambda_\mathrm{f}\lambda_k C_\rho \frac{\mathrm{e}^{\lambda_\delta\delta_y} - \mathrm{e}^{-\lambda_\delta\delta_y}}{\mathrm{e}^{\lambda_\delta\delta_y} + \mathrm{e}^{-\lambda_\delta\delta_y}}. \quad (15)$$

Defining $\theta_c = \arctan(C_h/\delta)$, the above equation can be rewritten as

$$\sqrt{\delta^2 + C_h^2}\sin(\theta - \theta_c) = \lambda_\mathrm{f}\lambda_k C_\rho \frac{\mathrm{e}^{\lambda_\delta\delta_y} - \mathrm{e}^{-\lambda_\delta\delta_y}}{\mathrm{e}^{\lambda_\delta\delta_y} + \mathrm{e}^{-\lambda_\delta\delta_y}}. \quad (16)$$

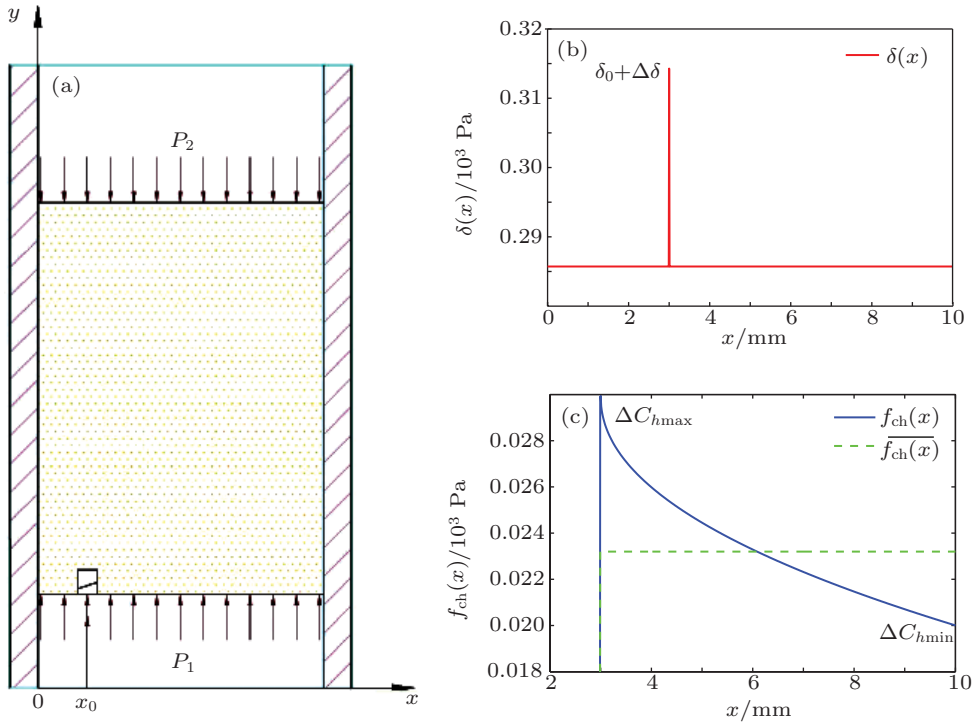


Fig. 2. (colour online) Stress distribution within mixed fluid flowing in a slot.

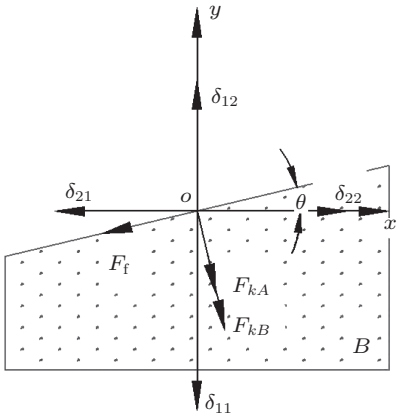


Fig. 3. Stress equilibrium analysis of the B phase.

Then the wedge angle can be obtained by solving Eq. (16) as follows:

$$\theta = \arcsin\left[\frac{\lambda_{\rm f}\lambda_k C_\rho}{\sqrt{\delta^2+C_h^2}}\frac{{\rm e}^{\lambda_\delta\delta_y}-{\rm e}^{-\lambda_\delta\delta_y}}{{\rm e}^{\lambda_\delta\delta_y}+{\rm e}^{-\lambda_\delta\delta_y}}\right]+\theta_c,$$
$$\theta\in\left[-\frac{\pi}{2},+\frac{\pi}{2}\right]. \tag{17}$$

It is clear that θ and θ_c indicate the moving trends of phase B in the longitudinal direction and in the transverse direction within the cell, respectively, so θ and θ_c are named the drift–inhibition angle and the expansion–inhibition angle, respectively, here.

Referring to the initial volume ratio of phase B in the cell before fluid flows as λ_0 and it is clear that $\lambda_0 = \Phi_B$, then the initial value of C_ρ, $C_{\rho 0}$, can be obtained by substituting λ_0 for λ in Eq. (7) as

$$C_{\rho 0} = \frac{\rho_A^2(1-\lambda_0)^2+\rho_B^2\lambda_0^2}{\rho_A(1-\lambda_0)+\rho_B\lambda_0)}. \tag{18}$$

Correspondingly, the initial drift–inhibition angle is

$$\theta_0 = \arcsin\left[\frac{\lambda_{\rm f}\lambda_k C_{\rho 0}}{\sqrt{\delta^2+C_h^2}}\frac{{\rm e}^{\lambda_\delta\delta_y}-{\rm e}^{-\lambda_\delta\delta_y}}{{\rm e}^{\lambda_\delta\delta_y}+{\rm e}^{-\lambda_\delta\delta_y}}\right]+\theta_c. \tag{19}$$

2.3. Discussion

Figure 4 shows the curve of C_p versus λ. Taking ${\rm d}(C_\rho)/{\rm d}\lambda = 0$ and solving Eq. (9), the inflection point of C_ρ curve can be obtained as

$$\lambda^* = \frac{\sqrt{2}\rho_A\rho_B-\rho_A\sqrt{\rho_A^2+\rho_B^2}}{(\rho_B-\rho_A)\sqrt{\rho_A^2+\rho_B^2}}, \tag{20}$$

where λ^* is the value of λ that satisfies ${\rm d}(C_\rho)/{\rm d}\lambda = 0$.

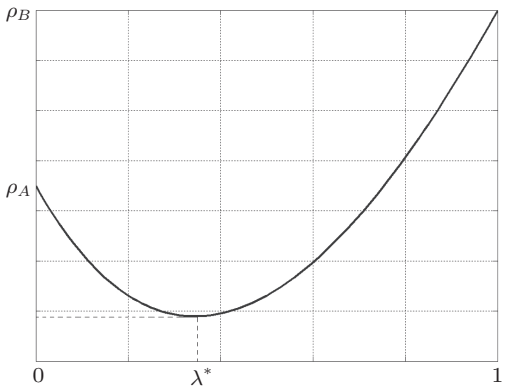


Fig. 4. Curve of C_p versus λ.

Because C_p reaches its minimum value at $\lambda = \lambda^*$ as shown in Fig. 4, and it is known from Eq. (17) that θ also arrives at its minimum value then, therefore λ^* is just the optimal volume ratio of phase B to the design volume of mixed fluid.

From the first part of right expression of Eq. (17) it follows that when $\lambda \in (0, \lambda^*)$, the drift of phase B will cause the value of C_p to increase, thus increasing the drift–inhibition angle and eventually leading the cell unit to reach its new stable state; when $\lambda \in (\lambda^*, 1)$, the drift of phase B will cause the value of C_p to decrease, thus reducing the drift–inhibition angle and eventually inducing more drift. So the volume of heavier ingredient should be designed to be $\Phi_B \leq \lambda^*$ in order to improve the stability of mixed fluid.

When the flow reaches its steady state and no transverse load exists, i.e., $C_h = 0$, substituting it into Eq. (17), the following equation will be obtained:

$$\theta = \arcsin\left[\frac{\lambda_{\rm f}\lambda_k C_\rho}{|\delta|}\frac{{\rm e}^{\lambda_\delta\delta_y} - {\rm e}^{-\lambda_\delta\delta_y}}{{\rm e}^{\lambda_\delta\delta_y} + {\rm e}^{-\lambda_\delta\delta_y}}\right]. \tag{21}$$

Obviously, θ is a decreasing function of $|\delta|$. From Eq. (17) it follows that when $\delta = 0$, there is no phase drift in the absence of applied pressure; when $\delta \to \infty$ then $\theta \to 0$, which means that there exists no interaction between the two phases, the stability of the mixed fluid is completely destroyed, then even a tiny stress gradient existing in the longitudinal direction will induce a serious phase drift.

Because θ_c is an increasing function of C_h, it is known according to the second part of right expression of Eq. (17) that the larger the value of C_h, the larger the value of θ will be, and then the different phases are easier to separate from each other and the mixed fluid becomes much more unstable.

3. Solving method on the model and its computing steps

Define the function

$$f(\delta,\theta) = \delta\sin\theta - C_h\cos\theta - \lambda_{\rm f}\lambda_k C_\rho\frac{{\rm e}^{\lambda_\delta\delta_y} - {\rm e}^{-\lambda_\delta\delta_y}}{{\rm e}^{\lambda_\delta\delta_y} + {\rm e}^{-\lambda_\delta\delta_y}}. \tag{22}$$

When the flow reaches its steady state and no transverse load exists, it is clear that $f(\delta,\theta) = 0$.

3.1. When a peak stress imposed

Supposing that there is a peak stress $\Delta\delta$ (N/mm^2) imposed on a cell at x_0 ($\Delta\delta \ll \delta$) and the number of the special cells on the x axis is S_i, which are shown in Figs. 2(a) and 2(b), correspondingly the initial parameters of cell S_i before the peak stress is imposed are λ_0 and θ_0, then the following equation is obtained by substituting them into Eq. (22)

$$\begin{aligned} f(\delta_i,\theta_i) &= (\delta+\Delta\delta)\sin\theta_0 - \lambda_{\rm f}\lambda_k C_\rho\frac{{\rm e}^{\lambda_\delta\delta_y} - {\rm e}^{-\lambda_\delta\delta_y}}{{\rm e}^{\lambda_\delta\delta_y} + {\rm e}^{-\lambda_\delta\delta_y}} \\ &= \Delta\delta\sin\theta_0 > 0. \end{aligned}$$

Because $f(\delta_i,\theta_i) > 0$, this extra lateral stress will lead the phase B of the specific cell to drift along the wedge surface, and then cause the volume ratio of phase B in the cell to decrease, eventually resulting in the decrease of θ_i according to Eqs. (18) and (19).

Supposing $\lambda_i = \lambda_i'$, the cell achieves its new equilibrium of stress $f(\delta_i,\theta_i') = 0$ through a time of phase drift, the new drift–inhibition angle can be calculated by Eq. (17) as

$$\theta_i' = \arcsin\left[\frac{\lambda_{\rm f}\lambda_k C_\rho}{\delta+\Delta\delta}\frac{{\rm e}^{\lambda_\delta\delta_y} - {\rm e}^{-\lambda_\delta\delta_y}}{{\rm e}^{\lambda_\delta\delta_y} + {\rm e}^{-\lambda_\delta\delta_y}}\right],$$

where $\lambda_i' < \lambda_0$ and $\theta_i' > \theta_0$.

The phase-drift of cell S_i will also cause the value of λ_{i+1} to increase and the stress balance in the adjacent cell S_{i+1} to be broken. For the same reason, the phase B of cell S_{i+1} will also drift in the same way. In a transversely unlimited space, the phases drift will take place in cells successively, and pushes the fluid to transversely expand unlimitedly. But in the slot, owing to the transverse restriction of the space, this drift motion will finally cease and meanwhile produce an extra transverse pressure imposed on the wall of slot. In addition, the Brownian motion of the fluid molecules will also drive the different ingredients to disperse continuously in the transverse direction and reach a balanced state.

So the phase drift which occurs in a single cell S_i will produce a chain of change of the component distribution in the mixed fluid. Defining the extra transverse expansion–inhibition force of cell S_i at x as $\Delta C_h(x)$, $x \in [x_0, H]$ and correspondingly the extra transverse pressure imposed on the wall of slot as $\Delta\delta_2$, then $\Delta\delta_2$ can be calculated as,

$$\Delta\delta_2 = \int_{x_0}^{H} \Delta C_h(x)\,\mathrm{d}x, \tag{23}$$

where H is the width of the slot (mm).

If the transverse size of cell is taken as $(H - x_0)$, i.e., the cell extracted is in the transverse section of mixed fluid, and the effects of the flow resistance and the plastic deformation of the cell are not taken into account, then the value of $\Delta\delta_2$ caused by peak stress can be obtained theoretically by substituting Eq. (23) into Eq. (15) as

$$\begin{aligned}\Delta\delta_2 \approx\ & \frac{1}{\cos\theta_0}\Bigg[(\delta + \Delta\delta)\sin\theta_0 \\ & - \lambda_{\mathrm{f}}\lambda_k C_{\rho 0}\frac{\mathrm{e}^{\lambda_\delta\delta_y} - \mathrm{e}^{-\lambda_\delta\delta_y}}{\mathrm{e}^{\lambda_\delta\delta_y} + \mathrm{e}^{-\lambda_\delta\delta_y}}\Bigg].\end{aligned} \tag{24}$$

From the above analysis and the definition of λ_δ it follows that the boundary conditions of function $\Delta C_h(x)$ are obtained as follows:

$$\begin{aligned}&\Delta C_{h\max} = \Delta C_h\,|_{x=x_0}\ , \quad \Delta C_{h\min} = \Delta C_h\,|_{x=}\,H\ , \\ &\frac{\Delta C_{h\max} - \Delta C_{h\min}}{\Delta C_{h\max}} = \lambda_\delta\frac{H - x_0}{H}.\end{aligned} \tag{25}$$

Because the variation of transverse expansion force within fluid is difficult to measure,[18] while the varying trend of $\Delta C_h(x)$ is clear, here we construct an exponential function to fit

$$\begin{aligned}\Delta C_h(x) =\ & \Delta C_{h\max} - (\Delta C_{h\max} - \Delta C_{h\min}) \\ & \times\left(1 - \frac{H - x}{H - x_0}\right)^{\lambda_\delta}.\end{aligned} \tag{26}$$

Substituting Eqs. (25) and (26) into Eq. (23), the following equation is obtained

$$\Delta C_{h\max} = \frac{H(\lambda_\delta + 1)\Delta\delta_2}{(H - x_0)(H + x_0\lambda_\delta)}. \tag{27}$$

Then substituting Eqs. (27), (25), and (24) into Eq. (26), ΔC_h can be calculated as

$$\begin{aligned}\Delta C_h \approx\ & \frac{H(\lambda_\delta + 1)}{(H - x_0)(H + x_0\lambda_\delta)} \\ & \times\left[1 - \frac{\lambda_\delta(H - x_0)^{1-\lambda_\delta}(x - x_0)^{\lambda_\delta}}{H}\right]\frac{1}{\cos\theta_0} \\ & \times\Bigg[(\delta + \Delta\delta)\sin\theta_0 - \lambda_{\mathrm{f}}\lambda_k C_{\rho 0} \\ & \times\frac{\mathrm{e}^{\lambda_\delta\delta_y} - \mathrm{e}^{-\lambda_\delta\delta_y}}{\mathrm{e}^{\lambda_\delta\delta_y} + \mathrm{e}^{-\lambda_\delta\delta_y}}\Bigg].\end{aligned} \tag{28}$$

Define the mean transverse expansion–inhibition force in the width direction of the slot as

$$\overline{C_h(x)} = \Delta\delta_2/(H - x_0).$$

The curve of ΔC_h under the action of a peak stress is shown in Fig. 2(c). The relevant data used in simulation here are as follows: $\delta_0 = 0.286 \times 10^3$ Pa, $H = 10$ mm, $x_0 = 3$ mm, and $\Delta\delta = \delta/10 = 0.0286 \times 10^3$ Pa.

In fact, component drift produces also a lengthways stress to the adjacent cells, which will cause the gradient variation of the flow velocity in the width direction of slot. Taking $\delta_0 = 0$, $x_0 = 0$, and $\Delta\delta = \tau$, the model can be regarded as a flat-flow model of non-Newtonian fluid, and as a special case, all the above formulas and conclusions also hold true.

3.2. When a gradient face stress imposed

Supposing that a gradient face stress is imposed on the end of mixed fluid, $\mathrm{d}\delta/\mathrm{d}x = f_\delta(x)$, $x \in (x_0, H)$, then the equivalent peak stress at x is

$$\delta(x) = \int_{x_0}^{x} f_\delta(t)\,\mathrm{d}t. \tag{29}$$

Substituting Eq. (29) into Eq. (28), the ΔC_h caused by the peak stress can be calculated from

$$\begin{aligned}C_h(x) \approx\ & \int_{x_0}^{x} f_{\mathrm{ch}}(t)\,\mathrm{d}t = \frac{H(\lambda_\delta + 1)}{(H - x_0)(H + x_0\lambda_\delta)} \\ & \times\left[1 - \frac{\lambda_\delta(H - x_0)^{1-\lambda_\delta}(x - x_0)^{\lambda_\delta}}{H}\right] \\ & \times\frac{1}{\cos\theta_0}\Bigg[\delta(x)\sin\theta_0 - \lambda_{\mathrm{f}}\lambda_k C_{\rho 0} \\ & \times\frac{\mathrm{e}^{\lambda_\delta\delta_y} - \mathrm{e}^{-\lambda_\delta\delta_y}}{\mathrm{e}^{\lambda_\delta\delta_y} + \mathrm{e}^{-\lambda_\delta\delta_y}}\Bigg].\end{aligned} \tag{30}$$

Substituting Eqs. (29) and (30) into Eq. (22), the following equation is obtained

$$\begin{aligned}&\delta(x)\sin\theta(x) - C_h(x)\cos\theta(x) \\ &\approx \lambda_{\mathrm{f}}\lambda_k C_\rho\frac{\mathrm{e}^{\lambda_\delta\delta_y} - \mathrm{e}^{-\lambda_\delta\delta_y}}{\mathrm{e}^{\lambda_\delta\delta_y} + \mathrm{e}^{-\lambda_\delta\delta_y}}.\end{aligned} \tag{31}$$

After deformation, we have

$$\begin{aligned}\theta(x) \approx\ & \arcsin\left[\frac{\lambda_{\mathrm{f}}\lambda_k C_{\rho 0}}{\sqrt{\delta(x)^2 + C_h(x)^2}}\frac{\mathrm{e}^{\lambda_\delta\delta_y} - \mathrm{e}^{-\lambda_\delta\delta_y}}{\mathrm{e}^{\lambda_\delta\delta_y} + \mathrm{e}^{-\lambda_\delta\delta_y}}\right] \\ & + \arctan\left(\frac{C_h(x)}{\delta(x)}\right).\end{aligned} \tag{32}$$

Utilizing the computer tools, the curve of $\theta(x)$ can be discretely drawn from Eq. (32), and then the drift trend of phase can be reflected by the variation of $\theta(x)$ in the x direction of x. And the mean lengthways force and the mean lateral expansion–inhibition force can also be respectively calculated as follows: $\overline{\delta(H)} = \int_{x_0}^{H} \delta(x)\mathrm{d}x/(H - x_0)$, and $\overline{C_h(H)} = \int_{x_0}^{H} C_h(x)\mathrm{d}x/(H - x_0)$.

Expanding C_ρ by Eq. (8) and eliminating C_ρ from Eq. (31), the following equation is obtained

$$\begin{aligned}&\frac{\rho_B^2+\rho_A^2}{(\rho_B-\rho_A)^2}[\rho_A+(\rho_B-\rho_A)\lambda]-\frac{2\rho_A\rho_B(\rho_B+\rho_A)}{(\rho_B-\rho_A)^2}\\&+\frac{2\rho_B^2\rho_A^2}{(\rho_B-\rho_A)^2}\frac{1}{[\rho_A+(\rho_B-\rho_A)\lambda]}\\=&\frac{\delta(x)\sin\theta(x)-C_h(x)\cos\theta(x)}{\lambda_{\mathrm{f}}\lambda_k}\frac{\mathrm{e}^{\lambda_\delta\delta_y}+\mathrm{e}^{-\lambda_\delta\delta_y}}{\mathrm{e}^{\lambda_\delta\delta_y}-\mathrm{e}^{-\lambda_\delta\delta_y}}.\end{aligned}$$

After deformation and classification, we have

$$\begin{aligned}&C_1(\lambda+C_2)-C_3+C_4\frac{1}{\lambda+C_2}\\=&\frac{\delta(x)\sin\theta(x)-C_h(x)\cos\theta(x)}{\lambda_{\mathrm{f}}\lambda_k}\frac{\mathrm{e}^{\lambda_\delta\delta_y}+\mathrm{e}^{-\lambda_\delta\delta_y}}{\mathrm{e}^{\lambda_\delta\delta_y}-\mathrm{e}^{-\lambda_\delta\delta_y}},\end{aligned}\tag{33}$$

where

$$\begin{aligned}C_1&=\frac{\rho_B^2+\rho_A^2}{\rho_B-\rho_A},\quad C_2=\frac{\rho_A}{\rho_B-\rho_A},\\C_3&=\frac{\rho_A^3-2\rho_A^2\rho_B-\rho_A\rho_B^2}{(\rho_B-\rho_A)^2},\quad\text{and}\\C_4&=\frac{2\rho_B^2\rho_A^2}{(\rho_B-\rho_A)^3}.\end{aligned}\tag{34}$$

The C_1–C_4 each are dependent on ρ_A and ρ_B.

Substituting the discrete value of $\theta(x)$ into Eq. (33) and solving the equation, the curve of $\lambda(x)$ can be discretely but qualitatively drawn and then its function can also be fitted by making use of the computer tools.

4. Application and the checking of the model

Grease is a kind of a typical multi-phase mixed fluid in which the heavier phases (such as the saponifier, densifier, additives, etc.) disperse into the lighter phase (the base oil). Our previous work[17] indicated that grease flowed with a velocity which had a gradient variation in the radial direction of pipe, and the front surface of the grease column bulged. Through the precise fitting and analysis, the shear stress function $\tau(r)$ in the radial direction is obtained as

$$\tau(r)=\frac{\tau_w}{R-r^*}(r-r^*),\tag{35}$$

where τ_w is the shearing stress on the inner wall of pipe (Pa); R is the radius of pipe (mm); r^* is the radius of the plug flow (mm); $r^* = 2\tau_y l/\Delta p$, with l being the length of the grease volume in the pipe (mm), and equal to the length of the pipe when grease is full of the pipe; τ_y is the yield stress of grease (Pa).

Eliminating r^* from Eq. (35), the shear stress function within grease in the radial direction is obtained as follows, and the curve of $\tau(r)$ varying with r is shown in Fig. 5.

$$\tau(r)=\begin{cases}\dfrac{\tau_w}{\Delta PR-2\tau_y l}(\Delta Pr-2\tau_y l), & r^*\le r\le R,\\ 0, & 0\le r<r^*.\end{cases}\tag{36}$$

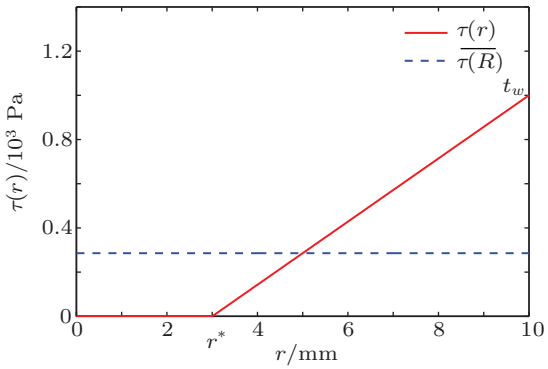


Fig. 5. (colour online) Distribution of $\tau(r)$ in the radial direction.

4.1. Application of the model

All the parameters of ρ_A, ρ_B, and Φ_A, Φ_B can be calculated respectively according to the relevant parameters of grease components. And substituting these relevant parameters into Eqs. (34), (18), and (3), C_1–C_4, $C_{\rho 0}$, and λ_δ can be obtained respectively. Measuring the value of δ_y by single-way compressing experiment, and substituting δ_y into Eq. (4), λ_k can be calculated.

Taking the base oil as phase A and the other ingredients as phase B, the researching cell extracted here is a micro-sector block. Taking the pipe radius as x axis and the pipe axis as y axis, a cylindrical coordinate system is established. Measuring the value of the radial pressure of grease upon the pipe wall δ_{g} (Pa) and noticing that $H = R$ and $x_0 = 0$, the distribution of the radial expansion–inhibition stress can be expressed by Eq. (28) as

$$C_h(r)=\frac{(\lambda_\delta+1)}{R}\left[1-\frac{\lambda_\delta R^{1-\lambda_\delta}r^{\lambda_\delta}}{R}\right]\delta_{\mathrm{g}}.\tag{37}$$

If the value of $\delta_{\rm g}$ is difficult to measure such as the flow of grease in a small pipe, etc., then it can be simply estimated through the following equation:

$$C_h(r) \approx \frac{(\lambda_\delta+1)}{R}\left[1-\frac{\lambda_\delta R^{1-\lambda_\delta} r^{\lambda_\delta}}{R}\right]\frac{1}{\cos\theta_0} \times\left[\tau(r)\sin\theta_0-\lambda_{\rm f}\lambda_k C_{\rho 0} \times\frac{{\rm e}^{\lambda_\delta\tau_y}-{\rm e}^{-\lambda_\delta\tau_y}}{{\rm e}^{\lambda_\delta\tau_y}+{\rm e}^{-\lambda_\delta\tau_y}}\right]. \quad (38)$$

The mean shear stress and the mean radial expansion–inhibition force are calculated respectively as

$$\overline{\tau(R)} = \int_0^R \tau(r)\,{\rm d}r/R = \frac{\tau_w(\Delta PR-4\tau_y l)}{2(\Delta PR-2\tau_y l)}, \quad (39)$$

$$\overline{C_h(R)} = \int_0^R C_h(r)\,{\rm d}r/R \approx \frac{(\lambda_\delta+1)}{R}\left[1-\frac{\lambda_\delta R^{1-\lambda_\delta} R^{\lambda_\delta}}{R}\right]\frac{1}{\cos\theta_0} \times[\overline{\tau(R)}\sin\theta_0-\lambda_{\rm f}\lambda_k C_{\rho 0} \times\frac{{\rm e}^{\lambda_\delta\tau_y}-{\rm e}^{-\lambda_\delta\tau_y}}{{\rm e}^{\lambda_\delta\tau_y}+{\rm e}^{-\lambda_\delta\tau_y}}]. \quad (40)$$

The internal maximum friction coefficient of grease $\lambda_{\rm f}$ is approximately taken to be the maximum static friction coefficient between two phases. If the gradient variation of stress is not taken into consideration, then it is deemed that the loading forces on the grease are only $\overline{\tau}(R)$ and τ_y. Because the resistance force of grease is always in the direction parallel to the axis of pipe but opposite to the direction of flow, the stress loading on the cell extracted anywhere should meet the following equation:

$$(F_{kA}+F_{kB})+F_{\rm f}=\overline{\tau(R)}-\tau_y. \quad (41)$$

Substituting Eqs. (1), (2), and (5) and $C_{\rho 0}$ into Eq. (41), the following equation is obtained

$$\lambda_k(\lambda_{\rm f}+1)C_{\rho 0}\frac{{\rm e}^{\lambda_\delta\tau_y}-{\rm e}^{-\lambda_\delta\tau_y}}{{\rm e}^{\lambda_\delta\tau_y}+{\rm e}^{-\lambda_\delta\tau_y}}=\overline{\tau(R)}-\tau_y.$$

From the above equation, we have

$$\lambda_{\rm f}=\frac{\overline{\tau(R)}-\tau_y}{\lambda_k C_{\rho 0}}\frac{{\rm e}^{\lambda_\delta\tau_y}+{\rm e}^{-\lambda_\delta\tau_y}}{{\rm e}^{\lambda_\delta\tau_y}-{\rm e}^{-\lambda_\delta\tau_y}}-1. \quad (42)$$

4.2. Simulation analysis of the ingredient distribution in grease

Substituting the above parameters into Eq. (37) or Eq. (38), the discrete values of the initial radial expansion–inhibition force $C_h(r)$ at the beginning of grease flowing in pipe can be calculated, and its curve can also be drawn by making use of computer tools as shown in Fig. 6. It is clearly known from Fig. 6 that the variation of $C_h(r)$ with r is the same as the variation of the distribution of $\tau(r)$ in the radial direction and its maximum value $C_h(R)$ occurs at the pipe wall.

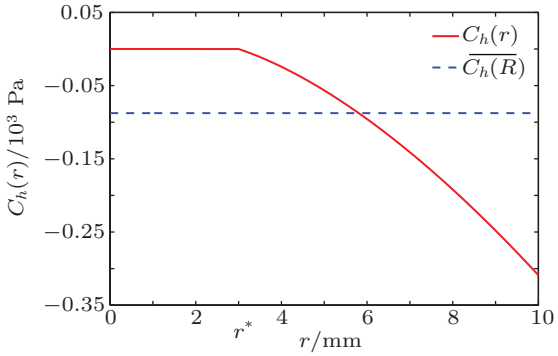


Fig. 6. (colour online) Initial distribution of $C_h(r)$.

Substituting the relevant parameters into Eq. (24), then the discrete values of the initial drift–inhibition angle $\theta(r)$ at the beginning of grease flowing in a pipe can be calculated, and its curve can be drawn by making use of computer tools as shown in Fig. 7. It can be known from the figure that $\theta(r)$ is a decreasing function of r, and its values at different r values indicate the drifting trend of heavier ingredient where it is clear that there is a biggest trend of the heavier ingredient to separate from the base oil near the wall, and the shear-thinning phenomenon is more apparent along the increasing direction of shear gradient.

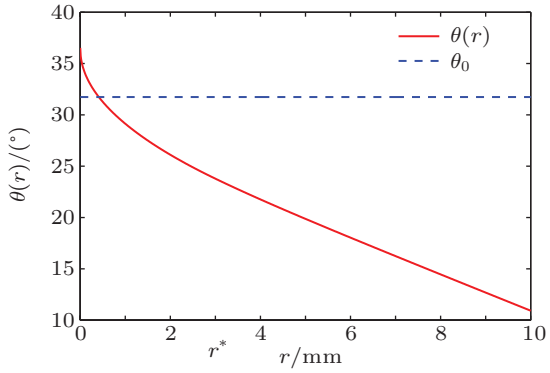


Fig. 7. (colour online) Initial distribution of $\theta(r)$.

Substituting the discrete values of $\theta(r)$ into Eq. (33) and solving the resulting equation, then the discrete value of $\lambda(r)$ when the flow of grease reaches its stable state can be calculated and its curve can be

drawn by making use of computer tools as shown in Fig. 8. It is known from the figure that the grease exhibits a rheological characteristic of Newtonian fluid near the wall of pipe because in the fluid there is almost a single-phase composition ($\lambda(r=0) \approx 0$). There is a plug flow area occurring within $r \in [0,3)$ and the radius of the pug flow decreases with the increase of ΔP, and the plug flow area will disappear completely when ΔP is bigger enough.

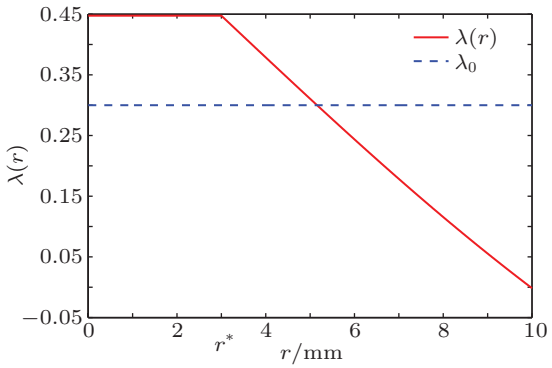


Fig. 8. (colour online) Distribution of $\lambda(r)$ when grease flows steadily.

The relevant data used in our simulation are as follows: $\Delta p = 18 \times 10^3$ Pa, $\tau_w = 1 \times 10^3$ Pa, $l = 100$ mm, $R = 10$ mm, $\rho_A = 1.8$ (g/cm^3), $\rho_B = 2$ (g/cm^3), $\phi_A = 0.7$, and $\phi_B = 0.3$. All of the parameters can be calculated or measured through relevant experiments, and the details of these experiments are presented in Ref. [18].

5. Conclusion

(I) Based on the minimum entropy theory of steady-state system, a two-phase wedge-sliding model is developed and used to describe the phenomena of the ingredient drift in mixed fluid in a non-uniform stress field. As an example, when it is used to describe the ingredient distribution of grease, the ingredient distribution in the grease presents a gradient along the varying direction of the stress when the flow reaches its stable state.

(II) The variables of drift–inhibition angle $\theta(x)$ and transverse expansion–inhibition angle $\theta_c(x)$ are put forward to index the drift trends of different ingredients in mixed fluid, which are respectively caused by the transverse gradient variation of stress $\delta(x)$ and the loading applied perpendicularly.

(III) The research results show that there exists an optimal volume ratio between heavier ingredient λ^* and the composition of mixed fluid. And the volume ratio of heavier ingredient Φ_B should be designed to be smaller than its λ^* so that the mixed fluid has better stability.

(IV) When the model is applied separately to the case of a peak stress and to the case of a gradient stress, the solving methods are illustrated and meanwhile their computing steps are given in details.

(V) Taking the grease flowing in a pipe as an example and applying this model, the phenomena of ingredient drift are studied. The simulation results show that the model can better reveal the ingredient distribution in grease when the flow reaches its stable state.

References

[1] Michael R K, David T L and Mark J M 1999 *Phys. Fluids* **11** 833
[2] Nouar C and Frigaard I 2009 *Phys. Fluids* **21** 064104
[3] Hatzikiakos S G and Dealy J M 1991 *J. Rheol.* **35** 497
[4] Tong Z H 2010 *Acta Phys. Sin.* **59** 1884 (in Chinese)
[5] Liu H T, Chang J Z , An K and Su T X 2010 *Acta Phys. Sin.* **59** 1877 (in Chinese)
[6] Blunt M, King M J and Scher H 1992 *Phys. Rev.* A **46** 7680
[7] Niessner J and Hassanizadeh S M 2008 *Water Resour. Res.* **44** W08439
[8] Pailha M and Pouliquen O 2009 *J. Fluid Mech.* **633** 115
[9] Ballesta P, Lettinga M P and Manneville S 2007 *J. Rheol.* **51** 1047
[10] Bossio B M, Blanco A J and Hernandez F H 1992 *ASME Fluids Engineering Division Summer Meeting*, Vail, Co. August 2–6, 2009 p. 525
[11] Cho Y I and Choi E 1993 *Tribol. T.* **4** 545
[12] Bustos M C, Concha F, Bürger R and Tory E M 1999 *Sedimentation and Thickening: Phenomenological Foundation and Mathematical Theory* (The Netherlands: Kluwer Academic Publishers) pp. 27–31
[13] Tudor A and Nasui G V 2000 *U. Politeh. Buch.* D **62** 51
[14] Higgins R V and Leighton A J 1962 *J. Petrol. Technol.* **14** 679
[15] Nott P R and Brady J F 1994 *J. Fluid Mech.* **275** 157
[16] Ali E A and Mohamed E O 2009 *Rheol. Acta* **48** 285
[17] Han Z H and Liu Z M 2011 *Adv. Sci. Lett.* **4** 830
[18] Xu G Y and Zhang Y Z 2005 *Study on Rheological and Transport Properties of Grease* (Nanjing: China University of Mining and Technology Press) pp. 53–66 (in Chinese)